LBL-19579

Lawrence Berkeley Laboratory
UNIVERSITY OF CALIFORNIA

Accelerator & Fusion Research Division

LBL--19579
DE85 015277

Presented at the 1985 Particle Accelerator Conference,
Vancouver, B.C., Canada, May 13-16, 1985

DESIGN AND PERFORMANCE OF 40 mm, 6.5 T, COLLARED, COLD-IRON MODEL MAGNETS

C. Peters, W. Gilbert, W. Hassenzahl, K. Mirk,
J. Rechen, R. Scanlan, and C. Taylor

May 1985

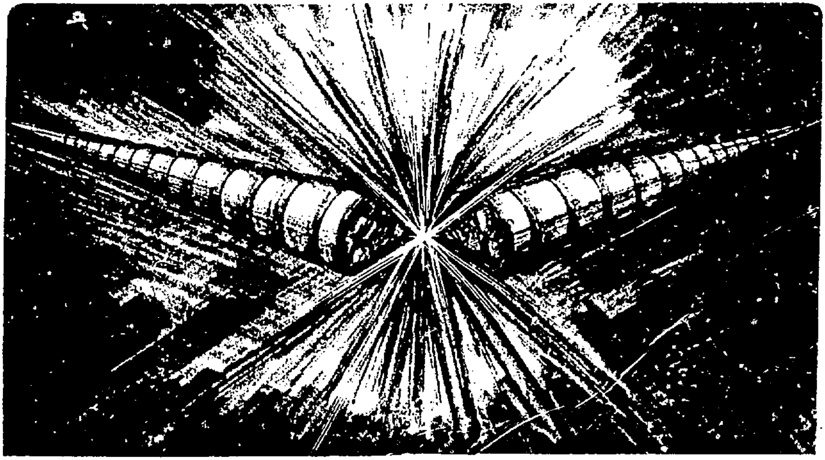

Prepared for the U.S. Department of Energy under Contract DE-AC03-76SF00098

LBL-19579

DESIGN AND PERFORMANCE OF 40 MM, 6.5 T, COLLARED, COLD-IRON MODEL MAGNETS*

C. Peters, W. Gilbert, W. Hassenzahl, K. Mirk, J. Rechen, R. Scanlan, and C. Talyor

Lawrence Berkeley Laboratory
University of California
Berkeley, California 94720

May 1985

---

* This work was supported by the Director, Office of Energy Research, Office of High Energy and Nuclear Physics, High Energy Physics Division, U.S. Dept. of Energy, under Contract No. DE-AC03-76SF00098.

DESIGN AND PERFORMANCE OF 40 MM, 6.5 T, COLLARED, COLD-IRON MODEL MAGNETS*

C. Peters, W. Gilbert, W. Hassenzahl, K. Mirk, J. Rechen, R. Scanlan, and C. Taylor
Lawrence Berkeley Laboratory
University of California
Berkeley, California 94720

Dipole Model Program

Model magnets have been built and tested at the Lawrence Berkeley Laboratory to verify a candidate design for the main bending magnets of the SSC. Construction of this series of dipole models was begun in October 1984 and will be completed in October 1985. To date, three models with collars, C1, C2, and C3, have been completed. Model C1 and C2 have been tested.

SSC Model Dipole

The inside diameter of the magnet winding is 1.574 inches (40 mm), which is the same as anticipated for the SSC itself. The overall length of the magnet is 41 inches and the straight section is 28 inches. The ends of the coils are flared for ease of winding.

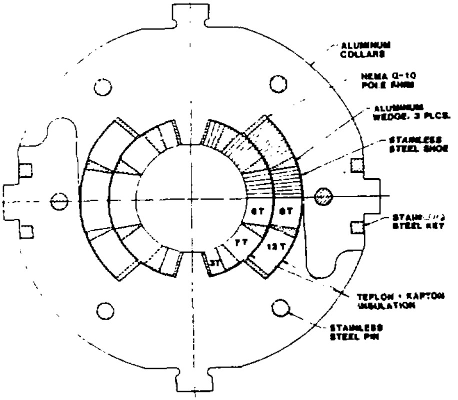

XBL 855-2358

Fig. 1 Model C1 and C3 Collared Coil Assembly

The cross section shown in Fig. 1 has been designated SSC reference design D. It consists of a two wedge, 16 turn inner layer and a one wedge, 20 turn outer layer. Kapton sheets provide insulation between layers and ground plane insulation from coil to collars.

Two flattened "keystoned" cables were developed for this design, described in Table I. The strand Jc (4.2 K, 5T) values for C1 are 2280 A/mm^2 (inner) and 2273 A/mm^2 (outer); for C-2 the values are 2238 A/mm^2 (inner) and 2435 A/mm^2; and for C-3 the values are 2500 A/mm^2 (inner) and 2435 A/mm^2 (outer). The cable is insulated with two spiral wraps of pre-epoxy coated kapton. The inner is 0.001 inch thick and the outer is 0.002 inch thick.

Table I

Superconducting Cable Description

Layer	Cable
Inner	23 strands of 0.0318 inch dia. NbTi wire, 1.3 Cu to S.C., 1.68° keystone
Outer	30 strands of 0.0255 inch dia. NbTi wire, 1.8 Cu to S.C., 1.24° keystone

Fig. 1 shows the aluminum collars used in model C1 and C3. Smaller stainless steel collars were used in model C2. Table II tabulates collar description. The collars are assembled into 6 inch long collar packs held together with 0.25 inch diameter pins. Two 0.187 inch square keys on each side lock mating collar packs around the compressed coil assembly. Die-stamped collars will be used in future models.

Table II

Model No.	Collar Mat'l	Collar Radial Thick.	Collar plate Thick.	Fabrication Method
C-1 & C-3	7075-T6 Aluminum	0.955 in.	0.125 in.	N.C. machined
C-2	Nitronic 40 S.S.	0.588 in.	0.065 in.	Laser cut

A "cold" iron yoke provides alignment of the collared coil assembly and magnetic flux return. The machined yoke blocks in the 28 inch center section are iron and the yoke blocks housing at the ends are aluminum. The yoke blocks are pinned to stainless steel assembly plates and the top and bottom yokes assemblies are bolted together with aluminum tie rods.

Due to the difficulty in forming cylindrical coil ends, the coil ends have been flared to a modified conical shape. This design satisfies the mechanical, electrical, and magnetic requirements for the magnet end. The overall end length is 6.12 inches and maximum diameter is 5.10 inches. Maximum conductor stress is reduced by increasing the conductor "hardway" bend radius in the end (i.e. bending in the plane of the cable flat face). This radius is larger than the flat cross section radius by 95% and 47% in layers 1 and 2, respectively.

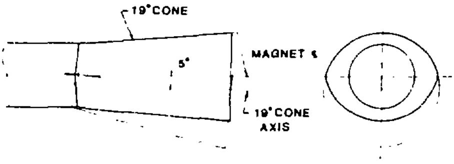

XBL 855-2355

Fig. 2 Magnet End Geometry

---

* This work was supported by the Director, Office of Energy Research, Office of High Energy and Nuclear Physics, High Energy Physics Division, U.S. Dept. of Energy, under Contract No. DE-AC03-76SF00098.

This shape also is very well suited for the coil forming process. Without additional clamping or support, the coil ends hold this "tilted" cone shape. In other words, the cable likes this shape. This minimizes motion and chafing of the cable during subsequent compression and curing. This permits winding the coils without additional turn to turn insulation in the ends. No electrical shorts occurred, in construction and testing of 3 dipole models. Finally, the gentle bending of the cable in the ends permits the assembled coils to be relatively free of out of position and poorly clamped strands.

Magnet Construction

Coil Forming

Prior to coil winding, the inner and outer cable were each accurately measured. For these initial models, correction "shims" of NEMA G-11 were then placed in the coil during winding to compensate for real cable size and to maintain the correct position of each conductor block. The cable is wound onto aluminum forms. At the ends, it makes a turn around a NEMA G-10 pole piece. The coils are compressed and heated in a curing fixture at 10,000 psi and 150°C, for about one hour. The conductor in the ends is compressed at the mid-plane but not axially toward the magnet center. After curing, each coil with its permanently affixed end pole piece was measured under load. Coil modulus after curing during its first compression cycle between 6,000 and 10,000 psi for the inner and outer coils was 1.38×10^6 psi and 1.15×10^6 psi, respectively.

Coil Assembly

The four cured coils were assembled onto a collapsible assembly mandrel. The coil ends were aligned with pins on a machined conical end form. This form also provided internal support. The coil ends were held down by an overwrap of 0.010 inch thick Kevlar braid. Teflon tape (0.002 inch thick) was butt wrapped over each entire layer, including the ends. Formed Kapton insulation pieces were then placed over each layer for layer to layer and coil to ground insulation. The Kapton pieces interleave at the magnet mid-plane. One significant difference between the three dipole models constructed was the thickness of Kapton between layers. Model C-1 and C-3 had no Kapton between layers and model C-2 had 0.015 inch of Kapton between layers. It appears that the Kapton between layers of model C-2 contributed to its considerable loss of prestress upon cooldown (see Fig. 4).

Coilaring

Prior to assembly, each of the four molded coils were measured in a compression fixture. These measurements were used to predict dimensions of pole shims to be used during assembly. Typically, due to the deformation of the collars and plastic components, a trial collaring of a 4 inch-long section was required. An adjustment was then made to the predicted pole shim thicknesses to achieve correct assembled coil pressures. The remaining collar packs were then assembled, two 6 inch long packs (12 inches total) to each side of center. The collars were assembled with a stainless steel shoe (0.024 inch thick) between the outer layer and the collars. During collaring the collars slide against the shoe rather than on the Kapton ground plane insulation. Typically the maximum pressure on the coils during collaring was about 2.5 times the pressure remaining after collaring. In other words, as the collaring press is released and the collars begin to support the coil force, the coil pressure drops by 60%. Collar deflections after collaring are shown in Table III.

Yoke Assembly

The collared coil assembly is transferred to the yoke assembly. A tapered insulator is fit over the coil ends. In the assembly, the end aluminum yoke blocks and tie rods provide the clamping force to compress the coil ends. The iron yoke blocks in the center straight section only position and align the collared coil to the iron center but do not provide any clamping. All coil to coil splices are made externally to the magnet ends.

Magnet Test Results

Instrumentation

Coil pressure data was obtained using strain gages in the center 4 inch-long collar pack. A portion of the collar plates were cut away and replaced with a block mounted with strain gages as shown in Fig. 3. The gages were calibrated prior to collaring the real magnet coils and were found to be insensitive to diameter changes and load applied to the other layer.

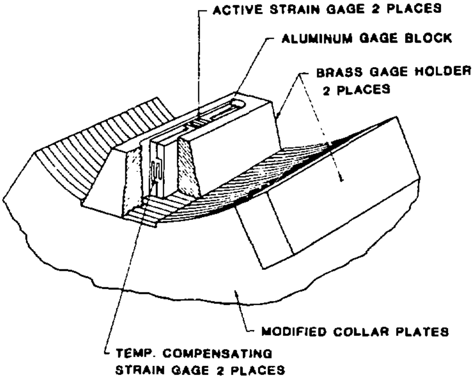

XBL 865-2364

Fig. 3 Pressure Gage Arrangement

Four coil position indicators (CPI's) were installed on the iron yoke assembly as a means of measuring collar position relative to the yoke during operation. Each CPI uses a cantilevered beam with 4 strain gages. The iron yoke with the 4 CPI's was set up and cooled to 77 K for calibration. A second test found that the CPI's accurately predict the thermal contraction of a mock aluminum collar installed in the yoke.

Collar Deflections

Collar deflections are summarized in Table III for assembly and cooldown and in Table IV for deflections during operation.

Coil Pressure

The increase in coil prestress in model C1 upon cooldown, seen in Fig. 4, as opposed to the loss of prestress in model C2, can be attributed largely to collar design and material. The large loss of prestress in the inner layer of C2 is further magnified by the radial thermal contraction of the Kapton insulation between layers in model C2. During operation, Fig. 5 shows that coil pressure at the poll of each layer of Model C1 decreases with successive quenches. After sufficient training, the coil pressure is reversible. This behavior reflects the presence of friction and the somewhat plastic nature of the coils.

Table III

Measured Collar Diameter Deflections during Assembly and Cooldown

Values are change in collar diameters x 0.001 inch and are positive for increasing diameter.

Model # & Collar Type		Undeflected Collar	Collared Magnet 300 K	Collared Magnet 4 K
C-1 Aluminum 25 mm	Vert.	0	+3	-13
	Horiz.	0	+2	-19
C-2 Nitronic 15 mm	Vert.	0	+5	-10
	Horiz.	0	+6	- 8
C-3 Aluminum 25 mm	Vert.	0	+10	
	Horiz.	0	+6	

Table IV

Measured and Predicted Collar Diameter Deflection During Operation

Values are change in collar diameters x 0.001 inch and are positive for increasing diameter. Values in ( ) are predicted deflections.

Model # & Collar Type		0amps.	3000 A	6000 A	8000 A
C-1 Aluminum 25 mm	Vert.	0	-0.5	-1.5(-3.2)	-2.7
	Horiz.	0	+0.3	+0.8(+1.6)	+1.8
C-2 Nitronic 15 mm	Vert.	0	-0.7	-2.3(-2.8)	
	Horiz.	0	+0.6	+3.3(+2.8)	
C-3 Aluminum 25 mm	Vert.	0			
	Horiz.	0			

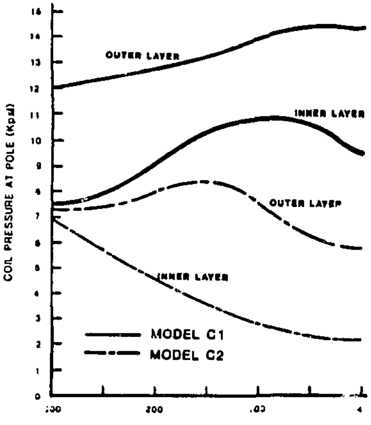

Fig. 4 Model C1 and C2 Coil Pressure During Cooldown

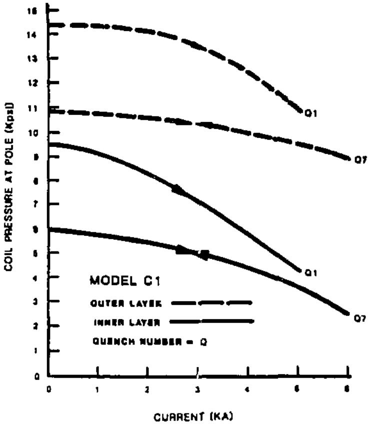

Fig. 5 Model C1 Coil Pressure During Operation

Training

The training behavior of Model C1 is shown in Fig. 6. The first quench occurred at 5.1 tesla and 6.1 tesla was achieved on the fourth quench, which is a rather good training curve. The magnet was warmed to room temperature and recooled to 4.4 K, training was resumed. Some of the memory was lost. In He II, 1.8 K, training to 8 tesla was very rapid. Short sample performance was achieved.

Training of Model C2 was excellent; 5.5 tesla on the first quench and 6.0 tesla on the second. This data was taken in a short preliminary test with a more extensive test program underway.

Magnetic Field Measurements

Both magnets' magnetic fields were measured with our rotating magnetic pickup coil system. Both the fields from transport current and from magnetization effects agree with our calculations.

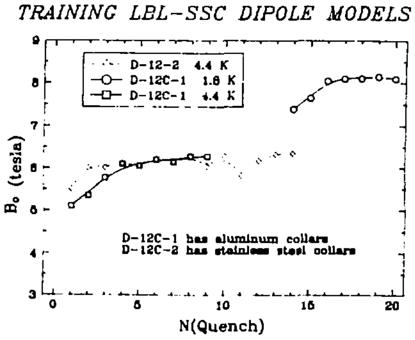

Fig. 6 Model C1 and C2 Training Behavior